Journal of Biomechanics 70 (2018) 26–32

Contents lists available at ScienceDirect

Journal of Biomechanics

journal homepage: www.elsevier.com/locate/jbiomech
www.JBiomech.com

# Biomechanical response of intact, degenerated and repaired intervertebral discs under impact loading – *Ex-vivo* and *In-Silico* investigation

Mohammad Nikkhoo [a], Jaw-Lin Wang [b,*], Mohamad Parnianpour [c], Marwan El-Rich [d], Kinda Khalaf [d,*]

[a] Department of Biomedical Engineering, Science and Research Branch, Islamic Azad University, Tehran, Iran
[b] Institute of Biomedical Engineering, College of Medicine and Engineering, National Taiwan University, Taipei, Taiwan, ROC
[c] Department of Mechanical Engineering, Sharif University of Technology, Tehran, Iran
[d] Department of Biomedical Engineering, Khalifa University of Science, Technology and Research, Abu Dhabi, United Arab Emirates

ARTICLE INFO

*Article history:*
Accepted 14 January 2018

*Keywords:*
Intervertebral disc
Degeneration
Genipin repair
Impact loading
*Ex-vivo* experiments
Finite element analysis

ABSTRACT

Understanding the effect of impact loading on the mechanical response of the intervertebral disc (IVD) is valuable for investigating injury mechanisms and devising effective therapeutic modalities. This study used 24 porcine thoracic motion segments to characterize the mechanical response of intact (N = 8), degenerated (Trypsin-denatured, N = 8), and repaired (Genepin-treated, N = 8) IVDs subject to impact loading. A meta-model analysis of poroelastic finite element simulations was used in combination with *ex-vivo* creep and impact tests to extract the material properties. Forward analyses using updated specimen-specific FE models were performed to evaluate the effect of impact duration. The maximum axial stress in the IVDs, Von-Mises stress in the endplates, and intradiscal pore pressure (IDP) were calculated, under a 400 N preload, subject to a sequence of impact loads for 10 impact durations (10–100 ms). The results were in good agreement with both creep and impact experiments (error < 10%). A significant difference was found in the maximum axial stress between the intact and degenerated disc groups. The IDP was also significantly lower in the degenerated disc group. The Von Mises stress in the adjacent endplates significantly increased with degeneration. It is concluded that the disc time-dependent response significantly changes with disc degeneration. Cross-linker Genipin has the potential to recover the hydraulic permeability and can potentially change the time dependent response, particularly in the IDP. This is the first study, to our best knowledge, which explores the effect of impact loading on the healthy, degenerated and repaired IVD using both creep and impact validation tests.



## 1. Introduction

Degeneration of the intervertebral disc (IVD), regardless of the phenotypes, risk factors and initiating mechanisms is directly linked to acute and chronic low back pain (LBP), the leading cause of disability worldwide (WHO, 2016). Degenerative disc disease (DDD) is estimated to afflict one third of the world's adult population, instigating significant morbidity and socioeconomic challenges, which are increasing as the elderly population continues to grow. The underlying causes for disc degeneration (DD) are multifactorial, where genetic and environmental factors, age, nutritional compromise, as well as mechanical loading history, all predispose the healthy disc to structural failure (Adams and Roughley, 2006; Dudli et al., 2012). It is widely accepted, though, that mechanical loading plays a key role in DD (Adams and Dolan, 2016).

Numerous theoretical, experimental, and computational studies have investigated the effect of mechanical loading on disc degeneration at the cervical, thoracic and lumbar levels (Dreischarf et al., 2016; Illien-Junger et al., 2010; Shirazi-Adl et al., 2016; Wilke et al., 1999). These studies considered multiple loading scenarios, including static/quasi-static loads, dynamic, and complex loading. Much less work, however, has been done on the effect of impact or fast rate loading on the spine, in part due to its lower prevalence during normal physiological activities and the complexity of studying impact trauma experimentally (Wagnac et al., 2011). In vitro animal models were used to characterize the response of

* Corresponding authors at: Department of Biomedical Engineering, Khalifa University of Science and Technology, PO. Box 127788, Abu Dhabi, United Arab Emirates (K. Khalaf). Institute of Biomedical Engineering, College of Engineering & College of Medicine, National Taiwan University, #1, Section 1, Jen-Ai Road, Taipei 100, Taiwan, ROC (J.-L. Wang).

*E-mail addresses:* jlwang@ntu.edu.tw (J.-L. Wang), kinda.khalaf@kustar.ac.ae (K. Khalaf).

https://doi.org/10.1016/j.jbiomech.2018.01.026
0021-9290/

DD following high impact trauma (Dudli et al., 2012; Haschtmann et al., 2006; Hsu et al., 2013). The important question of whether a single impact without structural endplate impairment is sufficient to promote DD was recently addressed using a full organ culture model (Dudli et al., 2014). High impact loading was reported to weaken disc tissue by disrupting the matrix structure and altering the gene expression profile, hence leading to degenerative changes and predisposing the disc for endplate fractures.

Various Finite Element Models (FEM) were also employed to investigate the response of the IVD to impact loading. Most were motivated by spinal trauma, common to high speed impact loads generated in motor vehicle crashes (MVCs), combat and military situations, or high impact sports (El-Rich et al., 2009; Lee et al., 2000; Marini et al., 2015; Mustafy et al., 2014; Mustafy et al., 2016). According to these works, the loading rate has a significant influence on the mechanical behavior of spinal structures. Lumbar spine investigations demonstrated a modified injury pattern at high loading rate (0.38 m/s) including burst fractures and neurological injury (Tran et al., 1995). Impact investigations of the ligamentous cervical C2-C3 functional spinal unit (FSU) demonstrated different response to impact load and load-sharing depending on the rate and direction of loading. Strain energy assessment indicated that endplates are at increased risk of injury under rapid compression (Mustafy et al., 2014; Mustafy et al., 2016). Under fast dynamic loading conditions (high-energy impact), the load rate dependency of the IVD material properties may play a critical role in the biomechanics of spinal trauma. However, most of the FE models in literature used material properties derived from quasi-static experiments, thus neglecting this dependency (Wagnac et al., 2011). None of these studies used impact experimental tests to validate their models; rather, they employed creep and quasi static analyses, which may have limited their fidelity. Another potential limitation is the use of a hyperplastic formulation, which is not faithful to the inherent viscoelastic/poroelastic nature of the IVD (Mustafy et al., 2014; Mustafy et al., 2016; Wagnac et al., 2011). Since the healthy IVD is a well-hydrated porous composite structure, poroelastic models are valuable for mimicking its behavior (Argoubi and Shirazi-Adl, 1996).

The duration of impact is also important but understudied. For short impact durations, the high dynamic stiffness increases the FSU's stability (El-Rich et al., 2009). The effect of impact duration on the intradiscal pressure (IDP) is controversial, where some studies reported no effect (Lee et al., 2000), while others found an increase in the IDP (El-Rich et al., 2009; Wang et al., 2008).

We have previously developed an efficient methodology combining poroelastic FE models with a meta-model analytical approach, based on *ex-vivo* experiments, to extract and quantify the mechanical properties of intact, degenerated and repaired discs. (Khalaf et al., 2017; Nikkhoo et al., 2015; Nikkhoo et al., 2017). This study extends our work by investigating the response of the intact, degenerated and repaired intervertebral disc to impact loading scenarios. More specifically, the objective of this study was twofold: first to develop and validate a specimen-specific finite element model of the intervertebral disc using *ex-vivo* experiments based on both creep and impact loading, and second, to characterize the mechanical response of the intact, degenerated, and repaired intervertebral disc under impact shocks of varying durations. This is the first study, to our best knowledge, which explores the effect of impact loading on the healthy, degenerated and repaired IVD.

## 2. Materials and methods

This study commenced with *ex vivo* experiments, where three disc groups were prepared: intact, degenerated (using Trypsin) and repaired (using Genipin) discs. Impact loading was then induced using a custom-made drop tower. An inverse poroelastic FE model was used to extract the mechanical properties of the three disc groups. Forward FE analyses based on updated specimen-specific FE models were subsequently performed to evaluate the effect of the impact duration on the biomechanical response of intact, degenerated and repaired IVDs. The details are described in the following sections:

### 2.1. Ex-vivo experiment

#### 2.1.1. Specimen preparation and culturing procedure

24 porcine thoracic intervertebral discs were harvested from fresh 6-months-old juvenile pig spines within 4 h of demise. The specimens were prepared in sterile conditions. Upon the removal of the posterior elements and muscle tissue, the upper and lower vertebral bodies were cut parallel to the endplates. All specimens were washed 3 times with phosphate buffered saline (PBS) (Biowest), 0.5% gentamicin, 0.5% amphotericin, and Betadine. The specimens were incubated in a custom-made culturing system, including a bio-reactor, a circulation nutrition mechanism, and a pneumatic system to mimic physiological diurnal loading. Each disc was placed in a transparent chamber, where the culture nutrition media (changed every 2–3 days) was circulated at a rate of 200 μL/min. Standard control conditions were implemented (37 °C, 95% relative humidity, 5% $CO_2$). a 16-h dynamic loading scenario (0.2–0.8 MPa, 0.2 Hz), followed by an 8-h rest period (0.2 MPa), was applied (Gantenbein et al., 2006). Our pilot study confirmed that the cell viability of the intact NP was 84.1% (±6.9%) on day 1 and 82.9% (±8.3%) on day 7, while the viability for the intact AF was 82.0% (±7.4%) on day 1 and 80.3% (±8.6%) on day 7, respectively (Hsu et al., 2013). This confirmed that no physical degradation of the specimens occurred during the incubation.

#### 2.1.2. Ex-vivo experimental tests

Three different disc groups, intact (I), degenerated (D), and repaired(R), were used in the *ex-vivo* experiments, where 8 specimens were included per group. The intact discs group (I) did not receive treatment. Disc degeneration in group (D) was simulated in two stages: 0.5 ml Trypsin solution (0.25%) was injected into the NP on the first day, to induce biochemical protein denaturation, followed by a mechanical injury using 4-h fatigue loading (Peak-to-Peak 190-to-590 N, 2.5 Hz) to disrupt the disc's fibrous structure. For the third group (R), one ml of Genipin (0.33%) was injected into the NP one day after the simulated degeneration. Upon a subsequent incubation of 7 days for all 3 groups, a 1 h 0.8 MPa unconfined creep test was performed to extract the mechanical properties (elastic modulus (E) and hydraulic permeability (k)). The discs were then kept at rest for 12 h under a 0.2 MPa compressive load to prevent over-swelling. A custom-made drop-tower apparatus was used to induce impact loading (Fig. 1). The average peak load during impulse was 1200 N, using shock absorbers to provide contact for 20 ms (Fig. 2). The displacement of the specimens was measured using a linear potentiometer (25 mm, Gefran). The discs were finally cut into 2 segments from the midline, where one half was assigned for measuring the water content, while the other was used for histological studies to verify the degeneration grade.

### 2.2. Poroelastic FE modeling and material identification

A general poroelastic Finite Element (FE) model of the intervertebral disc was previously developed by the authors (Nikkhoo et al., 2013a) in ABAQUS v6.9, and validated using human cadaveric experiments under static, quasi-static, and dynamic loadings (Heuer et al., 2007; Li, 1994; Nikkhoo et al., 2013a). The inferior

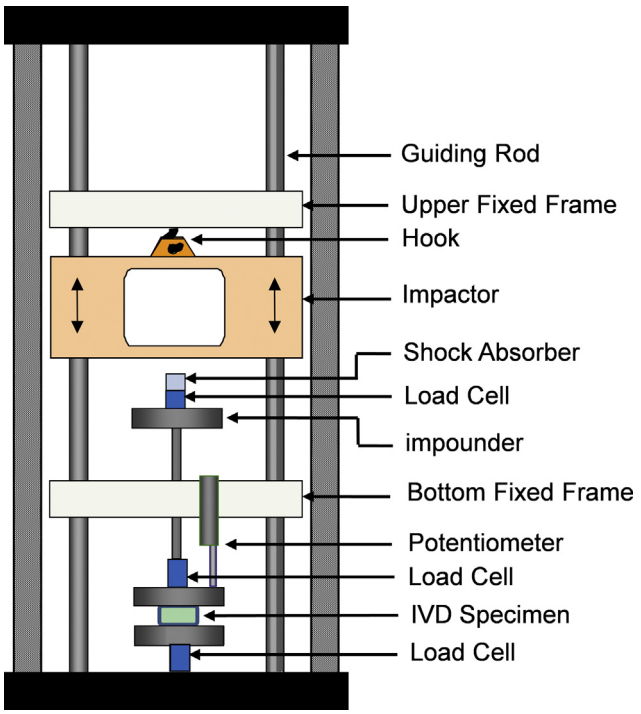


**Fig. 1.** Schematic of the impact test apparatus.

surface of the lower endplate was fixed as a boundary condition, while the axial displacement of the superior surface of the upper endplate was assumed constant. The fluid was free to flow in the NP, AF and endplates, although no element was allowed to slide along the interface of different materials. A UMAT code was developed to consider the strain-dependent permeability, which was assumed to depend on the void ratio (Argoubi and Shirazi-Adl, 1996). A constant boundary pore pressure (0.3 MPa) was imposed on the external surfaces to simulate the swelling phenomenon (Galbusera et al., 2011; Nikkhoo et al., 2015; Schmidt et al., 2011). Specimen specificity was implemented by using the measured radii and heights for all 24 discs to update the geometries of the associated FE models (Table 1). The void ratios of the discs were modified in the specimen-specific models based on the measured water content and related densities (Nikkhoo et al., 2013b; Nikkhoo et al., 2013c). Eight-node axisymmetric elements, with quadratic interpolation of the displacement field and linear interpolation of the pore pressure, were used to discretize the models. Large nonlinear deformations were used for the formulation, where the selected number of the nodes and elements were 19,916 and 6517, respectively, based on previous meshing sensitivity analyses (Nikkhoo et al., 2013a; Nikkhoo et al., 2011). Mimicking the experimental tests during quasi-static loading, a linear ramp function (0–0.8 MPa) was applied over 60 s on the superior surface of the model's upper endplate, followed by a 1 h unconfined creep. To simulate impact loading, a triangular impulsive force of 1200 N magnitude was applied to the upper endplate in the model for 20 ms.

A validated material identification algorithm, based on FE simulations and a quadratic response surface (QRS) regression model (Nikkhoo et al., 2013b), was used to identify optimal sets of the mechanical properties (i.e. E and k) for all 3 disc groups by linking the results of both creep and impact loading experiments with those obtained from the poroelastic FE simulations. To simplify the optimization procedure, Poisson's ratio was retained constant during the calculations based on our previous sensitivity analyses (Nikkhoo et al., 2013a; Nikkhoo et al., 2011; Nikkhoo et al., 2015). The ratio of the elastic modulus for the AF and NP was assumed to be 1.67, while the ratio of hydraulic permeability and Poisson's ratio of AF and NP was assumed to be 1 during the updating procedure (i.e. $k_{AF} = k_{NP}$, $E_{AF} = 1.67\ E_{NP}$) based on literature (Argoubi and Shirazi-Adl, 1996; Chagnon et al., 2010; Malandrino et al., 2009). The material properties of the adjacent endplates, maintained constant during the calculations, were obtained from literature. A Full-Factorial methodology was used for the design of experiments (DOE) in MATLAB (Mathworks). Two independent variables, (E) and (k), with six levels resulted in 72 simulations for each specimen (36 creep and 36 impact loading). The ranges of the independent variables for the I, D, and R disc groups were

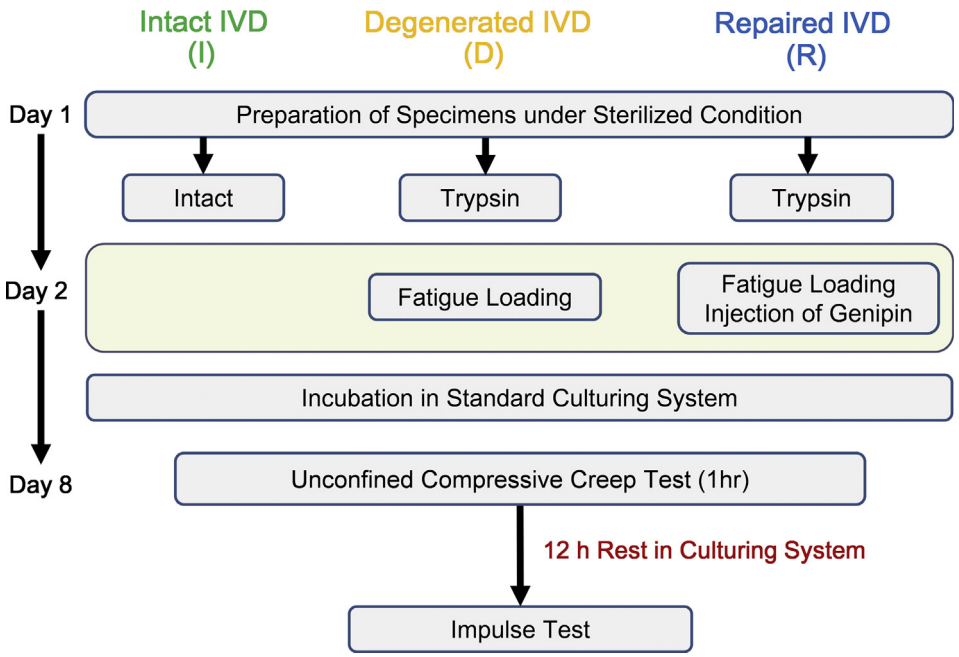


**Fig. 2.** Protocol of the *ex-vivo* experiments for 3 disc groups.

**Table 1**
Average disc height, radius, and porosity of Intact (I), Degenerated (D), and repaired (R) porcine intervertebral discs (N = 24). The reported values are in format of "Mean (±Standard Deviation)".

| Disc Group | Intact (I) | Degenerated (D) | Repaired (R) |
|---|---|---|---|
| Disc Height (mm) | 4.3 (±0.23) | 2.8 (±0.33) | 3.21 (±0.23) |
| Disc Radius (mm)* | 13.02 (±2.39) | 13.66 (±1.86) | 12.87 (±2.43) |
| Porosity of AF | 0.81 (±0.04) | 0.73 (±0.03) | 0.79 (±0.06) |
| Porosity of NP | 0.91 (±0.04) | 0.81 (±0.06) | 0.90 (±0.02) |

* The radius was calculated as the geometric average of the long and short axes of the disc.

initially guessed based on previous parametric studies (Nikkhoo et al., 2013b). The initial ranges of the modulus (E) were set to 2–3 MPa and 1.2–1.8 MPa, for the AF and NP, respectively, while the permeability (k) range was set to 1–3 $\times 10^{-16}$ $m^4$/Ns for both the AF and NP. The root mean square (RMS) errors were calculated to evaluate the correlations between the *ex-vivo* experiments and the FE-simulated disc responses in both creep and impact loading scenarios. A quadratic response surface (QRS) model was also constructed for each of the specimens, based on 72 sets of RMS errors and the input parameters (E and k). The optimized material properties were subsequently identified by minimizing the RMS errors using a direct search optimization procedure in MATLAB. The resulting optimal material properties were then entered into the FE model, such that if the RMS% was less than 10%, the calculated properties were considered accurate. For specimens with error larger than 10%, the calculated properties were adopted as center points, and new independent parameters were selected (Fig. 3).

### 2.3. FE simulations based on updated specimen-specific FE models

Upon the extraction of material properties in the 3 groups, the updated specimen-specific FE simulations were run subject to impact loading. The models were used to calculate the axial stress and intradiscal pore pressure in response to a sequence of impact loads during 10 different durations (10–100 ms). Impact tests were generated as triangular waveforms with a displacement of 1 mm, where a 400 N preload was used to simulate the body weight. The axial stress in the adjacent endplates was evaluated.

### 2.4. Statistical analysis

The material identification algorithm was used to extract the mechanical parameters. The differences in the elastic modulus and hydraulic permeability between different groups (intact, degenerated and repaired discs) were compared using one-way ANOVA (SPSS, Chicago). A linear discriminant analysis was initially performed to determine how well the combinations of the elastic modulus and permeability were able to classify the specimens in correct groups. Considering both parameters (i.e. E and k) in the discriminate analysis, the probability of correct classification using the FE meta-model was 87.5% (21 discs out of 26 discs). The simulation results of the axial stress, intradiscal pore pressure, and axial stress in the adjacent endplates were also compared using one-way ANOVA. The differences were considered to be significant at a P value < .05.

## 3. Results

The specimen-specific FE simulations were in good agreement with the *ex-vivo* experiments for all groups. Subject to creep, the average normalized percentages of the RMS errors were 5.07 (±1.52)%, 6.35 (±1.36)%, and 6.81 (±1.40)% for the intact, degenerated and repaired discs, respectively. Similarly, the average normalized percentages of the RMS errors were 6.69 (±1.79)%, 8.34 (±1.52)%, and 7.07 (±1.91)% for intact, degenerated and repaired discs, respectively, subject to impact loading.

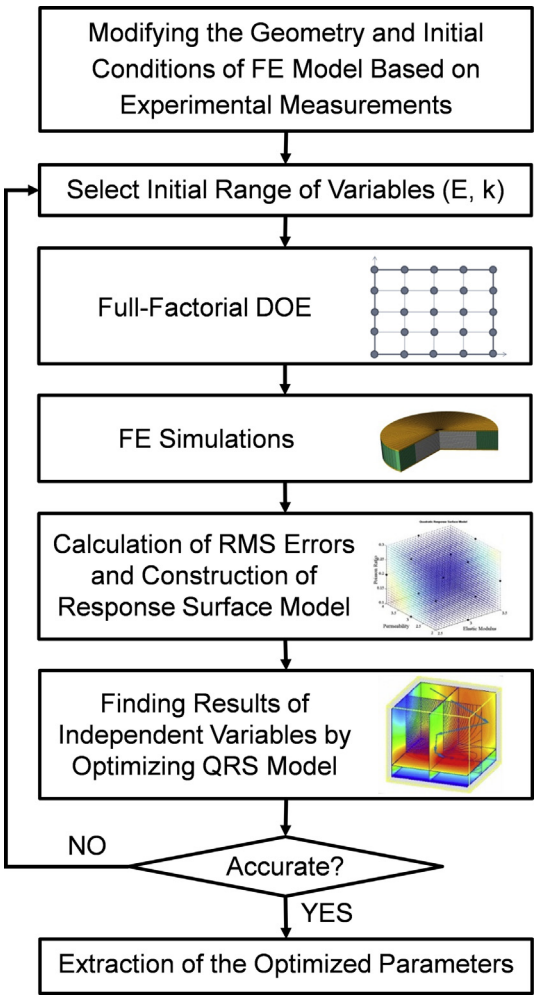


**Fig. 3.** Flowchart of material property identification protocol.

For the intact disc group, the average elastic moduli of the AF and the NP were 2.42 (±0.25) and 1.45 (±0.15) MPa, respectively, while the hydraulic permeability was 2.21 (±0.35) $\times 10^{-16}$ $m^4$/Ns. For the degenerated disc group, the average elastic moduli of the AF and the NP were 2.72 (±0.21) and 1.63 (±0.13) MPa, respectively, while the hydraulic permeability was 1.52 (±0.28) $\times 10^{-16}$ $m^4$/Ns. The comparative statistical analyses showed that the elastic modulus significantly increased for the degenerated group, in contrast to the hydraulic permeability, which significantly decreased (Fig. 4). For the repaired group, the elastic moduli of the AF and the NP were 2.58 (±0.19) and 1.55 (±0.11) MPa, respectively, and the hydraulic permeability was 1.92 (±0.31) $\times 10^{-16}$ $m^4$/Ns. The comparative statistical analyses revealed that the hydraulic permeability significantly increased as compared to the degenerated group, while the elastic modulus did not show significant changes (Fig. 4). Meanwhile, no significant differences were observed for the elastic modulus between the intact and repaired disc groups (Fig. 4).

The results of the specimen-specific FE simulations subject to impact loading for 20 ms showed a significant difference in the maximum axial stress between the intact and degenerated groups (Fig. 5). The intradiscal pore pressure was significantly lower in the degenerated group as compared to the intact (Fig. 5).

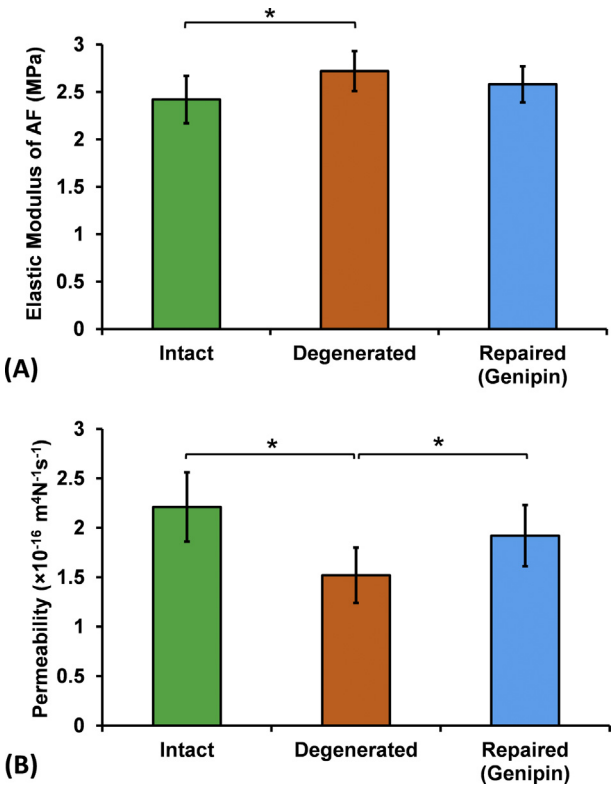


**Fig. 4.** Effect of degeneration and Genipin repaired on the disc (A) elastic modulus and (B) hydraulic permeability. *P value < .05. The error bars indicate the standard deviation.

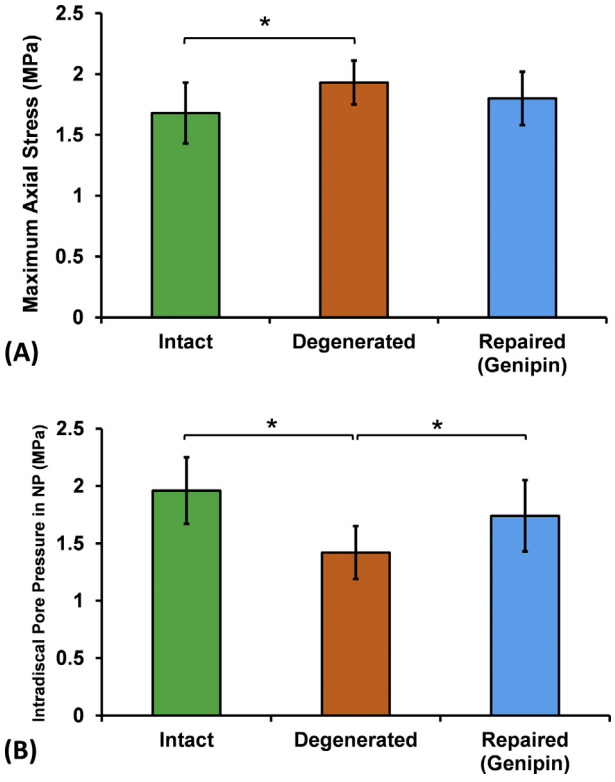


**Fig. 5.** Effect of degeneration and Genipin repaired on the disc (A) Maximum axial stress and (B) Intradiscal pore pressure in NP. *P value < .05. The error bars indicate the standard deviation.

Further simulations confirmed that the difference of the intradiscal pore pressure was significant for all impact durations, in comparison with the variation of the axial stress for all groups (Figs. 6 and 7). The time-dependent response, however, was more apparent in the intact and repaired groups (Figs. 6,7). The axial stress in the adjacent endplates significantly increased in the degenerated group, which may be a marker for the initiation of structural failure for the IVD (Fig. 8). The cross-linker, Genipin, enhances the structural integrity/interconnection of the AF, leading to better water retention and improved nucleus pore pressure (Fig. 7). This helps recover the dynamic properties of the IVD (Fig. 8).

## 4. Discussion

Understanding the role of impact loading on the spine is relevant due to the high energy released in a short period of time affecting various spinal structures and predisposing the IVD to premature degeneration and fracture. In literature, there is a paucity of data on the response of the IVD to impact loads, be it during rare abnormal occurrences in physiological activities, or as a result of

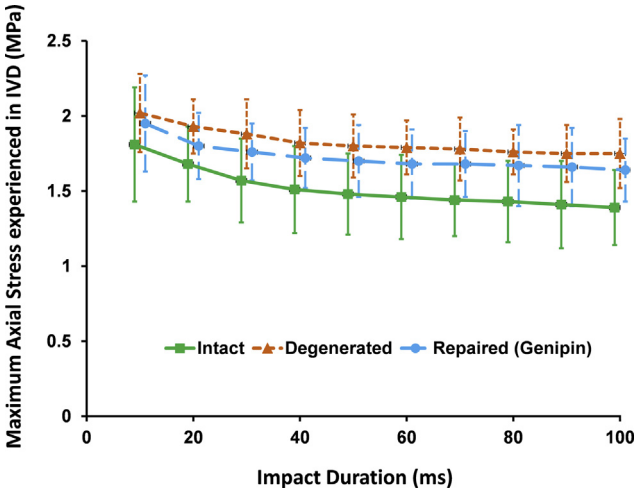


**Fig. 6.** The effect of impact duration on the maximum axial stress in IVD for intact, degenerated, and Genipin repaired discs. The error bars indicate the standard deviation.

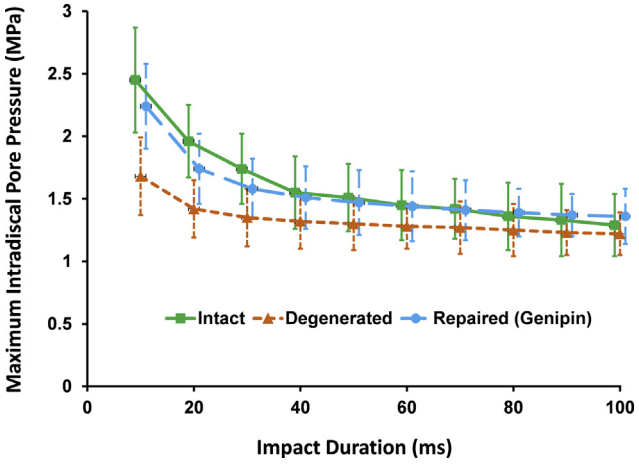


**Fig. 7.** The effect of impact duration on the intradiscal pore pressure in NP for intact, degenerated, and Genipin repaired discs. The error bars indicate the standard deviation.

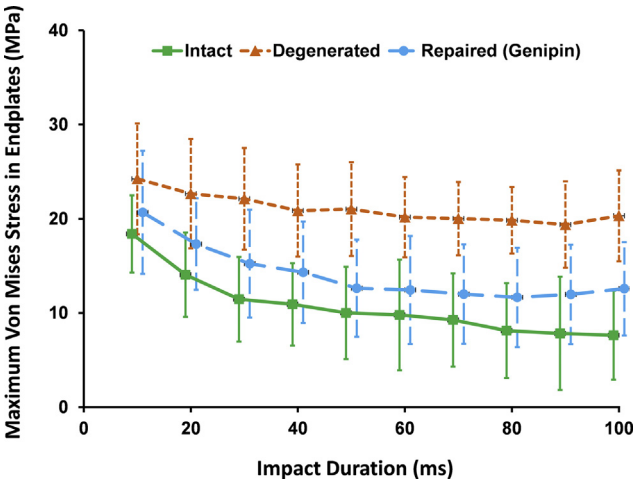


**Fig. 8.** The effect of impact duration on the Von Mises stress in adjacent endplates for intact, degenerated, and Genipin repaired discs. The error bars indicate the standard deviation.

high velocity trauma associated with motor vehicle accidents, military/combat situations, or impact sports.

This study investigated the effect of impact loading and its duration on intact, degenerated, and repaired IVDs to explore the influence of the loading rate on the mechanical behavior of the spinal structures and changes in injury patterns throughout the entire intact/degeneration/repair spectrum.

Applying impact loading on collapsed DD is postulated to disturb the extracellular matrix and disrupt the already disordered structure (Dudli et al., 2012). The pores are squeezed, which also aggravates the disc collapse. The IVD loses a significant percentage of water, leading to a stiffer solid phase with higher elastic modulus and axial stress. The stiffer tissue (both NP and AF) substantially restricts the fluid flow, potentially leading to decreased hydraulic permeability and lower intradiscal pore pressure.

Previous work including ours demonstrated that although Genipin improves the retention of the proteoglycans in repaired IVDs and minimizes the collapse of the collagen fibers, therefore slightly decreasing the elastic modulus, it is unable to reverse the modulus back to its intact value (Hsu et al., 2012; Hsu et al., 2013; Nikkhoo et al., 2017). In this study, the IVD regained some water content, which we hypothesize is due to the increased proteoglycans, hence enhancing the fluid flow. The hydraulic permeability increased upon Genepin injection, increasing the intradiscal pore pressure to approximately the same level of intact discs. It is hypothesized in this study that Genepin restores the mechanical integrity/competence of the ECM, leading to better retention of the hydrophilic proteoglycans and hence improved disc hydration.

The model prediction of an almost constant maximum axial stress for degenerated and repaired IVDs, independent of impact duration, suggests that the stress mainly depends on the magnitude of the compressive force rather than the rate of impact. However, the axial stress in the intact group exhibited slight time dependency. The variation of the intradiscal pore pressure was found significant during different impact durations, in comparison with the variation of the axial stress, in all three groups. The time-dependent response, however, was more significant in the intact and repaired groups, suggesting that disc degeneration has more influence on the IVD damping coefficient rather than its stiffness. Further work is needed for validation.

Our results confirm the presence of greater stresses in the adjacent endplates during impact loading in alignment with literature (Dudli et al., 2012; Dudli et al., 2016). The axial stress in the adjacent endplates significantly increased for the degenerated group, implying a potential endplate-driven failure process initiation.

Some limitations should be considered when interpreting the results. First, the axisymmetric FE models are a simplification of the actual non-symmetric geometry and do not reflect the non-heterogeneous mechanical properties. The models did not incorporate the posterior elements or facet joints given the large number of simulations (around 2300) involved. The posterior components were also removed during the *ex-vivo* experiments to minimize cost (media/incubator space), and to lessen contamination/infection risk. It is important to note that although we consider the model adequate since only axial compressive loading was applied experimentally, future work should explore better representative models. The second limitation was assuming a constant ratio for the elastic moduli and permeability of the AF and NP in all groups based on available data in literature (Argoubi and Shirazi-Adl, 1996; Schmidt et al., 2010). This reduced the number of independent variables. Elsewise, 4 independent variables would increase the simulations from 36 to 1296, and the simulations/ specimen from 72 to 2592. The use of harvested intervertebral discs of juvenile pigs instead of human IVDs is another limitation. Human cadaveric discs are more difficult to obtain and maintain logistically and are much more costly. Although the mechanical properties of porcine IVDs are different from human discs, they are frequently used in relevant studies as a suitable animal model (Beckstein et al., 2008; McLain et al., 2002). For future investigations, human cadaveric discs are recommended.

This is the first study, to our best knowledge, which explores the effect of impact loading on the healthy, degenerated and repaired IVD using both creep and impact validation tests. Endplate-driven failures were found likely to occur under shorter impact, in alignment with literature, where axial stress provides a potential mechanical marker for failure initiation. The IVD time-dependent response significantly changes with disc degeneration. Cross-linker Genipin has the potential to recover the hydraulic permeability and can change the time dependent response of IVD, particularly the intradiscal pore pressure.

## 5. Conflict of interest

The authors declare that this study research was conducted in the absence of any commercial or financial affiliations that could be construed as a potential conflict of interest.

## References

Adams, M.A., Dolan, P., 2016. Lumbar intervertebral disc injury, herniation and degeneration. In: Pinheiro-Franco, J.L., Vaccaro, A.R., Benzel, E.C., Mayer, M. (Eds.), Advanced Concepts in Lumbar Degenerative Disk Disease. Springer-Verlag, Berlin Heidelberg.

Adams, M.A., Roughley, P.J., 2006. What is intervertebral disc degeneration, and what causes it? Spine 31, 2151–2161.

Argoubi, M., Shirazi-Adl, A., 1996. Poroelastic creep response analysis of a lumbar motion segment in compression. J. Biomech. 29, 1331–1339.

Beckstein, J.C., Sen, S., Schaer, T.P., Vresilovic, E.J., Elliott, D.M., 2008. Comparison of animal discs used in disc research to human lumbar disc: axial compression mechanics and glycosaminoglycan content. Spine 33, E166–E173.

Chagnon, A., Aubin, C.E., Villemure, I., 2010. Biomechanical influence of disk properties on the load transfer of healthy and degenerated disks using a poroelastic finite element model. J. Biomech. Eng. 132, 111006.

Dreischarf, M., Shirazi-Adl, A., Arjmand, N., Rohlmann, A., Schmidt, H., 2016. Estimation of loads on human lumbar spine: a review of in vivo and computational model studies. J. Biomech. 49, 833–845.

Dudli, S., Ferguson, S.J., Haschtmann, D., 2014. Severity and pattern of post-traumatic intervertebral disc degeneration depend on the type of injury. Spine J.: Official J. North Am. Spine Soc. 14, 1256–1264.

Dudli, S., Haschtmann, D., Ferguson, S.J., 2012. Fracture of the vertebral endplates, but not equienergetic impact load, promotes disc degeneration in vitro. J. Orthop. Res.: Official Publ. Orthop. Res. Soc. 30, 809–816.

Dudli, S., Liebenberg, E., Magnitsky, S., Miller, S., Demir-Deviren, S., Lotz, J.C., 2016. Propionibacterium acnes infected intervertebral discs cause vertebral bone

marrow lesions consistent with Modic changes. J. Orthop. Res.: Official Publ. Orthop. Res. Soc. 34, 1447–1455.
El-Rich, M., Arnoux, P.J., Wagnac, E., Brunet, C., Aubin, C.E., 2009. Finite element investigation of the loading rate effect on the spinal load-sharing changes under impact conditions. J. Biomech. 42, 1252–1262.
Galbusera, F., Schmidt, H., Noailly, J., Malandrino, A., Lacroix, D., Wilke, H.J., Shirazi-Adl, A., 2011. Comparison of four methods to simulate swelling in poroelastic finite element models of intervertebral discs. J. Mech. Behavior Biomed. Mater. 4, 1234–1241.
Gantenbein, B., Grünhagen, T., Lee, C.R., van Donkelaar, C.C., Alini, M., Ito, K., 2006. An in vitro organ culturing system for intervertebral disc explants with vertebral endplates: a feasibility study with ovine caudal discs. Spine 31, 2665–2673.
Haschtmann, D., Stoyanov, J.V., Ferguson, S.J., 2006. Influence of diurnal hyperosmotic loading on the metabolism and matrix gene expression of a whole-organ intervertebral disc model. J. Orthop. Res.: Official Publ. Orthop. Res. Soc. 24, 1957–1966.
Heuer, F., Schmitt, H., Schmidt, H., Claes, L., Wilke, H.-J., 2007. Creep associated changes in intervertebral disc bulging obtained with a laser scanning device. Clin. Biomech. 22, 737–744.
Hsu, Y.-C., Chuang, I.T., Lin, J.-H., Nikkhoo, M., Chang, Y.-C., Wang, J.-L., 2012. Assessment of exogenous crosslinking therapy for biochemical and mechanical induced degeneration. J. Biomech. 45, S617.
Hsu, Y.-C., Kuo, Y.-W., Chang, Y.-C., Nikkhoo, M., Wang, J.-L., 2013. Rheological and dynamic integrity of simulated degenerated disc and consequences after cross-linker augmentation. Spine 38, E1446–E1453.
Illien-Junger, S., Gantenbein-Ritter, B., Grad, S., Lezuo, P., Ferguson, S.J., Alini, M., Ito, K., 2010. The combined effects of limited nutrition and high-frequency loading on intervertebral discs with endplates. Spine 35, 1744–1752.
Khalaf, K., Nikkhoo, M., Kargar, R., Najafzadeh, S., 2017. The effect of needle puncture injury on the biomechanical response of intervertebral discs. Bone Joint J. Orthop. Proc. Suppl. 99-B, 122-122.
Lee, C.K., Kim, Y.E., Lee, C.S., Hong, Y.M., Jung, J.M., Goel, V.K., 2000. Impact response of the intervertebral disc in a finite-element model. Spine 25, 2431–2439.
Li, S., 1994. Response of Human Intervertebral Disc to Prolonged Axial Loading and Low-Frequency Vibration [Doctoral Dissertation]. University of Illinois at Chicago, Department of Mechanical Engineering, Chicago IL.
Malandrino, A., Planell, J.A., Lacroix, D., 2009. Statistical factorial analysis on the poroelastic material properties sensitivity of the lumbar intervertebral disc under compression, flexion and axial rotation. J. Biomech. 42, 2780–2788.
Marini, G., Huber, G., Puschel, K., Ferguson, S.J., 2015. Nonlinear dynamics of the human lumbar intervertebral disc. J. Biomech. 48, 479–488.
McLain, R.F., Yerby, S.A., Moseley, T.A., 2002. Comparative morphometry of L4 vertebrae: comparison of large animal models for the human lumbar spine. Spine 27, E200–E206.
Mustafy, T., El-Rich, M., Mesfar, W., Moglo, K., 2014. Investigation of impact loading rate effects on the ligamentous cervical spinal load-partitioning using finite element model of functional spinal unit C2–C3. J. Biomech. 47, 2891–2903.
Mustafy, T., Moglo, K., Adeeb, S., El-Rich, M., 2016. Injury mechanisms of the ligamentous cervical C2–C3 functional spinal unit to complex loading modes: finite element study. J. Mech. Behavior Biomed. Mater. 53, 384–396.
Nikkhoo, M., Haghpanahi, M., Parnianpour, M., Wang, J.-L., 2013a. Dynamic responses of intervertebral disc during static creep and dynamic cyclic loading: a parametric poroelastic finite element analysis. Biomed. Eng.: Appl. Basis Commun. 25, 1350013.
Nikkhoo, M., Haghpanahi, M., Wang, J.L., Parnianpour, M., 2011. A poroelastic finite element model to describe the time-dependent response of lumbar intervertebral disc. J. Med. Imaging Health Inform. 1, 246–251.
Nikkhoo, M., Hsu, Y.-C., Haghpanahi, M., Parnianpour, M., Wang, J.-L., 2013b. A meta-model analysis of a finite element simulation for defining poroelastic properties of intervertebral discs. Proc. Instit. Mech. Eng. Part H: J. Eng. Med. 227, 672–682.
Nikkhoo, M., Hsu, Y.C., Haghpanahi, M., Parnianpour, M., Wang, J.L., 2013c. Material property identification of artificial degenerated intervertebral disc models—comparison of inverse poroelastic finite element analysis with biphasic closed form solution. J. Mech. 29, 589–597.
Nikkhoo, M., Khalaf, K., Kuo, Y.-W., Hsu, Y.-C., Haghpanahi, M., Parnianpour, M., Wang, J.-L., 2015. Effect of degeneration on fluid–solid interaction within intervertebral disk under cyclic loading–a meta-model analysis of finite element simulations. Front. Bioeng. Biotechnol. 3.
Nikkhoo, M., Wang, J.L., Abdollahi, M., Hsu, Y.C., Parnianpour, M., Khalaf, K., 2017. A regenerative approach towards recovering the mechanical properties of degenerated intervertebral discs: genipin and platelet-rich plasma therapies. Proc. Instit. Mech. Eng. Part H J. Eng. Med. 231, 127-137.
Schmidt, H., Galbusera, F., Wilke, H.J., Shirazi-Adl, A., 2011. Remedy for fictive negative pressures in biphasic finite element models of the intervertebral disc during unloading. Comp. Methods Biomech. Biomed. Eng. 14, 293–303.
Schmidt, H., Shirazi-Adl, A., Galbusera, F., Wilke, H.-J., 2010. Response analysis of the lumbar spine during regular daily activities—a finite element analysis. J. Biomech. 43, 1849–1856.
Shirazi-Adl, A., Schmidt, H., Kingma, I., 2016. Spine loading and deformation - from loading to recovery. J. Biomech. 49, 813–816.
Tran, N.T., Watson, N.A., Tencer, A.F., Ching, R.P., Anderson, P.A., 1995. Mechanism of the burst fracture in the thoracolumbar spine. The effect of loading rate. Spine 20, 1984–1988.
Wagnac, E., Arnoux, P.J., Garo, A., El-Rich, M., Aubin, C.E., 2011. Calibration of hyperelastic material properties of the human lumbar intervertebral disc under fast dynamic compressive loads. J. Biomech. Eng. 133, 101007.
Wang, J.L., Wu, T.K., Lin, T.C., Cheng, C.H., Huang, S.C., 2008. Rest cannot always recover the dynamic properties of fatigue-loaded intervertebral disc. Spine 33, 1863–1869.
WHO, 2016. World Health Statistics 2016.
Wilke, H.J., Neef, P., Caimi, M., Hoogland, T., Claes, L.E., 1999. New in vivo measurements of pressures in the intervertebral disc in daily life. Spine 24, 755–762.